ANALYSIS OF VULNERABILITY OF BUILDINGS DAMAGED AS A RESULT OF TERRORIST ATTACK: SCENARIO OF NON-LINEAR ANALYSES AND MULTI-CRITERIA OPTIMIZATIONS

Radomir Folić
University of Novi Sad
Faculty of Technical Sciences
Novi Sad, Serbia

Mladen Ćosić
Institute for testing of materials
Belgrade, Serbia

KEYWORDS: non-linear analysis, scenario, accidental actions, damage coefficient, multi-criteria optimization

ABSTRACT

The paper develops and presents a new multi-disciplinary methodology for the analysis of vulnerability of buildings exposed to accidental actions due to a terrorist attack. The methodology is based on *Non-linear Static Pushover Analyses* (NSPA) taking into account the principles of *Performance-Based Design* (PBD). The stiffness matrix for the impact of vertical actions has been used as the initial stiffness matrix in the non-linear analysis which is used to simulate the collapse of individual ground floor columns, forming several possible scenarios. The stiffness matrix by the end of the analysis which simulates the collapse of individual columns is used as initial stiffness matrix in *Non-Linear Static Pushover Analysis*. The building's vulnerability has been analyzed based on the calculated global and inter-storey drift, newly developed damage coefficient, and multi-criteria optimization. Prompt, reliable and sufficiently accurate answer can be obtained by using newly developed damage coefficient at the level of entire building in the capacitive domain, from elastic through non-linear and up to the collapse state. On the other hand, the damage scenario which requires priority and/or emergency repairs has been identified using the PROMETHEE multi-criteria optimization and considering the predefined alternatives and criteria. When linking different scientific disciplines (non-linear numerical analyses, failure analyses and multi-criteria optimization) qualitative and quantitative decisions can be made about the vulnerability of buildings with several optimized aspects.

INTRODUCTION

The behaviour of buildings in which a specific emergency situation occurred due to an act of terrorism, which is usually manifested in local damage or collapse of certain structural elements, indicates a possible progression of damage, including the collapse of the whole system. Given that multi-storey reinforced concrete buildings are statically undetermined systems, they are able to adapt to changes in a static system resulting from the effects of a terrorist act by redistributing the load and plasticizing their elements. The assessment of condition and the cause of collapse of the whole system or a part of it can be obtained using non-destructive testing, calculations or applying forensic engineering, based on which the new structural systems, elements and joints can be improved.

The complex engineering problem of analyzing the conditions/state of damaged buildings requires experts i.e. engineers with huge experience in assessing the state of buildings. In practice, the initial assessment of damage to structures is usually empirically-based with a qualitative description of their state, followed by a quantitative description using linear numerical models and dimensioning according to the regulations. However, the latest non-linear structural analysis software and the emerging designing methodologies using *Performance-Based Design* (PBD), indicate the possibility for reliable and multi-parameter approach in assessing the structure's state. Generally, the level of damage to structures can be assessed based on the following: simplified analysis, analytical procedures, energy criteria, damage index, calculating system performance using *Performance-Based Plastic Design* (PBPD), fragility curves, numerical one step solution, incremental-iterative analysis, *Non-linear Static Pushover Analysis* (NSPA), *Non-linear Dynamic Analysis* (NDA) and *Time-History Analysis* (THA).

The above analyses have been calculated using, among other things, numerical methods, including the *Finite Element Method* (FEM), *Discrete Element Method* (DEM), and the *Applied Element Method* (AEM). The assessment of system robustness under the effects of explosion based on modelling the effect by the sudden collapse of columns using the FEM is presented in (Zolghadr et al., 2012). In addition to the development of the system's non-linear behaviour, modelling the effect of explosion at the local level (column) also enables to establish a relation and consider the progressive collapse of the entire building. Papers (Ngo et al., 2007), (Makovička & Makovička Jr., 2014) and (Karlos & Solomos, 2013) presents the general approaches to effects of explosives to buildings in time domain, various numerical models of structures, and methods for simulating the effects of explosive. The response of the system to the blast effect in time domain has also been analyzed using methods which consider the system response in capacitive domain (Silva et al., 2005). Recent studies in the assessment of structures damaged as a results of a terrorist attack (the impact of explosives on the structure) are based on the integration of various scientific disciplines with the aim of considering all relevant system parameters in a comprehensive manner and making decisions on measures of structural repair/reinforcement. The paper (Stewart et al., 2006) develops a probabilistic risk assessment procedure in order to predict the risk of possible damage under a blast effect. Here, the concept of risk transfer has also been included, along with comparisons with natural hazards. The final solutions are shown using fragility curves and blast reliability curves. Given the almost ever-present budget restriction in funding structural repair, it is necessary to decide on priorities for repair and choosing the method of restoration of damaged buildings. The solution for these problems can be sought through the application of methods of *Multi-Criteria Decision Making* (MCDM). Today, there are a considerable number of multi-criteria decision making methods where the solution to the problem is obtained by choosing the best alternative from a set of predefined alternatives (*multi-attribute decision making*) or by programming the best alternative (*multi-objective decision making*) (Kabir et al., 2014). Among the methods of MCDM the following are the most widely used: TOPSIS (*Technique for Order Preference by Similarity to Ideal Solution*), CP (compromise programming), VIKOR (multi-criteria measure for compromise ranking), ELECTRA (*ELimination Et Choix Traduisant la REalité*), and PROMETHEE (*Preference Ranking Organization Method of Enrichment Evaluations*).

This paper describes a procedure of simulating the scenarios of interrelated analyses, providing thereby a better insight in the building's state and facilitating decisions on necessary interventions of the building. On the example of a ten storey reinforced concrete building, a procedure has been developed for determining the adaptability in accidental situations of the system. Given the fact that the PBD methodology requires system performance to be considered using non-linear numerical models bringing the system into a pre-collapse or collapse state, these advanced procedures enable the aforementioned decisions about the building to be highly reliable.

SCENARIO OF RELATED NON-LINEAR ANALYSES

The concept of the scenario of related non-linear analyses, presented in this research and in (Ćosić & Folić, 2015) is based on determining the structural condition while observing the *Performance-Based Design* (PBD) principles. The classical approach in the assessment of a damaged structure starts from the non-destructive methods, sample taking, empirical assessment and design of structures using linear analyses. The ultimate limit state and service life calculations are conducted according to the regulations, with contemporary European code (EN 1990:2002/A1:2005, 2005), (EN 1991-1-7:2006, 2006), (EN 1992-1-1:2004, 2004). In comparison to the European regulations, the American regulations (BIPS 05, 2011) and (UFC, 2013) consider the assessments of conditions and repair of the structures, which were exposed to accidental action in detail using the non-linear analyses. However, they do not take in consideration other accidental actions and relatedness of numerical models before and after sustaining damage. For the purpose of clearer defining and more accurate calculation of such complex problem, the scenario of related non-linear analyses is developed, which must be performed in order to make adequate decisions on the condition of the structure. In figure 1 is presented a flow chart of scenarios of the related non-linear analyses. In the first part, the calculation is conducted implementing the *Linear Static Analysis* (LSA) and *Spectral-Modal Analysis* (SMA). Further, by designing in compliance with (EN 1992-1-

1:2004, 2004) and (EN 1998-1:2004, 2004) codes, the necessary reinforcement in RC cross-sections is determined. In the second part a new 3D model of building is created for the non-linear analysis. At the first step of the second part, the static effects in the cross-sections of the structures are calculated only for vertical gravity actions (dead, super dead, live and similar loads). The system stiffness matrix at the end of this analysis is used as the initial stiffness matrix in the *Non-linear Static Pushover Analysis* (NSPA) for bidirectional pushover load (X and Y directions), which is conducted in the second step of the second part. As a non-linear response of the system the pushover curves, target displacement, forces and moments in cross sections, global drift (*DR*) and inter-storey drifts (*IDR*) are obtained.

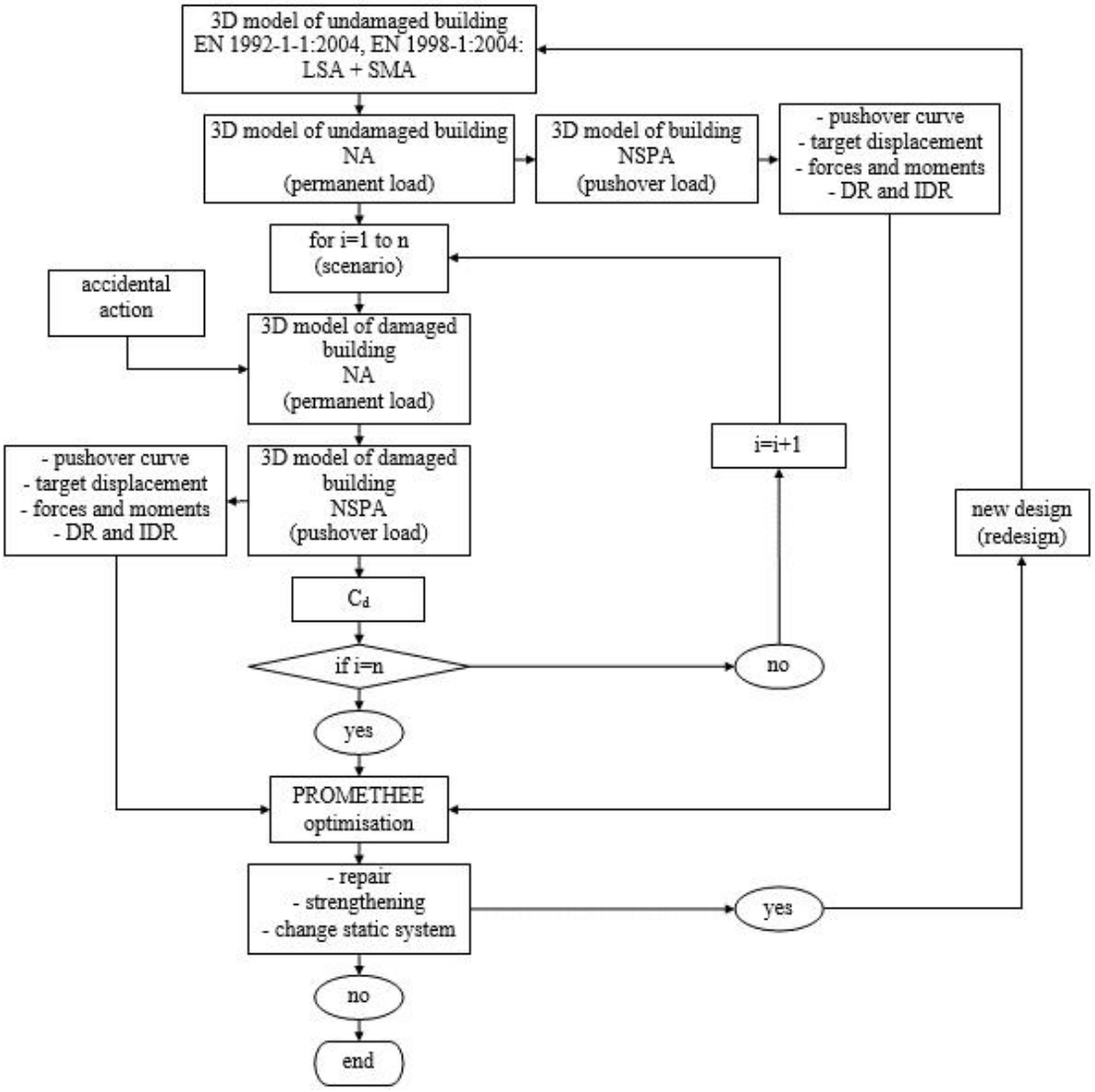

Figure 1. Flow chart of scenarios of the related non-linear analyses and optimization

In the third part, the simulation of accidental action on the structure is conducted, so the action causing decreases of bearing capacity, stability and serviceability of individual columns. The system stiffness matrix of the previous analysis is used as initial stiffness matrix of the non-linear analysis (NA) which simulates structural damage. The mathematical formulation for analyzing accidental action is derived based on the expression for the state of the undamaged building:

$$[K_0]\{D_0\} = \{P_0\}, \tag{1}$$

where $[K_0]$ is the stiffness matrix of the undamaged building, $\{D_0\}$ is the displacement vector of the undamaged building and $\{P_0\}$ is the load vector of the undamaged building. For the *i*-th damage scenario, the analysis is conducted based on:

$$[K_i]\{D_i\} = \{P_i\}, \quad [K_i] = [K_0] - [K_i'], \quad [M_i] = [M_0] - [M_i'], \tag{2}$$

where $[K_i]$ is the stiffness matrix of the damaged building, $\{D_i\}$ is the displacement vector of the damaged building, $\{P_i\}$ is the load vector of the damaged building, $[K_i']$ is the stiffness matrix of eliminated columns, $[M_i]$ is the mass matrix of the damaged building, $[M_0]$ is the mass matrix of the undamaged building and $[M_i']$ is the mass matrix of eliminated columns. In this case, development of non-linear strains in the system can be monitored, as well as the redistribution of static influences in the system. It is of particular importance that such analysis can serve for monitoring of plastic strain in the zone of severely damaged columns, i.e. monitoring of development of plastic hinges on the beams that are located in the local collapse zone. The number of possible scenarios *n* of structural damage and collapse of individual columns can be considerable. In the fourth part, the system stiffness matrix at the end of the structural damage analysis is used as initial stiffness matrix of NSPA analysis for bidirectional pushover load (X and Y direction), whereby the pushover curves are obtained as non-linear responses of the system, as well as target displacement, forces and moments in cross-sections, global *DR* and inter-storey drifts *IDR*. In the fifth section, the damage coefficient C_d has been calculated for each scenario and pushover load (X and Y directions) individually. Decisions regarding the possible need for repairing, reinforcing or partially changing the building's static system in the zone of collapsed columns are made based on calculated pushover curves, global *DR* and inter-storey *IDR* drifts, established fracture mechanisms and damage coefficient C_d upon the completion of the calculation on all pre-defined scenarios. The next step consists of optimization using the PROMETHEE method in order to decide which of the damage scenarios requires urgent repair and provide a better insight for creating a repair/strengthening strategy for of the building. If it is necessary to conduct some of the proposed procedures, the structure is redesigned, and possibly the procedure is reiterated for the purpose of verification and comparison of the obtained solutions. As it can be noticed, the calculation of the damaged structure conceived in this manner, simulates the realistic behaviour in the conditions of action and of accidental situation and pushover loads, by firstly exposing the structure to the action of the gravitational load, and then by exposing the structure loaded in this way to the accidental action. After that, the vulnerability of the structure is verified on the deformed and damaged structure, while the gravitational load is just transferred from the initial analysis to the following ones, and the accidental and pushover load are defined in the corresponding analyses.

DAMAGE COEFFICIENT

Considerations regarding the degree of damage to the building exposed to accidental and pushover loads were carried out by introducing the damage coefficient C_d (Ćosić & Folić, 2015). This is the coefficient based on which a comparative analysis between the undamaged and the damaged building is carried out. Unlike the existing damage indices, which are based on analyzing the degree of damage to the building subjected to external action and considering the system response in the time domain, the damage coefficient C_d approach considers the system response in the capacitive domain. Thus, a more complete picture can be obtained of the damage degree to the building, since it considers the system from its initial state through the non-linear elastic state to the collapse state. However, when considering the damage degree in the capacitive domain using the damage coefficient C_d, it is possible to cover all levels of capacity demand. The term on which the damage coefficient C_d was introduced is based on the comparative analysis of pushover curves of the undamaged and damaged building. Damage to the building, as already mentioned, are due to the action of an accidental situation and pushover load. For the purposes of this study, the damage coefficient C_d is defined based on the tri-linear pushover curve model, the reliability of which is sufficient to be applied in almost all non-linear responses of multi-storey buildings. Pushover curves of real building models are obtained by connecting a number of discrete values derived from incremental non-linear situations. The connection is carried out by using linear or spline interpolation, so that in the latter case the pushover curve leaves the impression of a smooth curve. Applying the tri-linear pushover curve model enables either to tri-linearize the pushover curve of the real building model or to take the pushover curve of the real building model as a basis for identifying the key parameters used as inputs for the tri-linear pushover curve model.

In order to conduct the parametric analysis, pushover curves are defined as a function of ductility coefficient μ and the ratio of the total base shear force of the building and the total base shear force of the building at the yield limit V/V_y (the relative total base shear force of the building). Parameters relevant to the tri-linear pushover curve model are the following:

- node 1: $0 \leq \mu_0 < 1$, $0 \leq (V/V_y)_0 < 1$,
  As a consequence of the previous accidental action or pushover load, the initial ductility coefficient μ_0 and the initial relative total base shear force of the building (V/V_y) can be non-zero, i.e. larger than zero and lower than 1.
- node 2: $\mu_y=1$, $(V/V_y)_y=1$,
  The ductility coefficient at the yield limit μ_y and the relative total base shear force of the building at the yield limit (V/V_y) are always equal to 1.
- node 3: $1 < \mu_{h/s} < \mu_{max}$, $(V/V_y)_{h/s} > 0$,
  The ductility coefficient for the level of hardening/softening $\mu_{h/s}$ is always higher than 1 and lower than the coefficient of maximum realized ductility μ_{max}, while the relative total base shear force of the building for the level of hardening/softening $(V/V_y)_{h/s}$ is higher than 0.
- node 4: $\mu_{max} > 1$, $(V/V_y)_{adeq} \geq 0$,
  The coefficient of the maximum realized ductility μ_{max} is always higher than 1, while the adequate relative total base shear force of the building $(V/V_y)_{adeq}$ is higher or equal to 0.

The damage coefficient C_d is generally defined as a function of absolute coordinate values, but for the purpose of parametric analysis, diagrams of pushover curves are presented as a function of relative coordinate values. Taking into account the previously derived positions on key parameters of the tri-linear pushover curve, but translated into absolute coordinate values, the following damage coefficient C_d is derived (Ćosić & Folić, 2015):

$$C_d = 1 - 0.125 \left[\frac{\int_0^{D_{maxd}} V_d(D_d)dD}{\int_0^{D_{maxu}} V_u(D_u)dD} + \frac{K_{i,d}}{K_{i,u}} + \frac{K_{n,d}}{K_{n,u}} + \frac{V_{y,d}}{V_{y,u}} + \frac{V_{h/s,d}}{V_{h/s,u}} + \frac{D_{maxd}}{D_{maxu}} + \frac{V_{adeq,d}}{V_{adeq,u}} + \frac{\mu_{maxd}}{\mu_{maxu}} \right]. \quad (3)$$

The damage coefficient C_d consists of eight important factors defining the degree of damage to the building by comparing the pushover curves of the undamaged and damaged building:

- determining the degree of damage based on the ratio of the pushover curve surface of the undamaged $\int V_u(D_u)dD$ and the damaged building $\int V_d(D_d)dD$,
- determining the degree of damage based on the ratio of initial stiffness of the undamaged $K_{i,u}$ and the damaged building $K_{i,d}$,
- determining the degree of damage based on the ratio of non-linear stiffness of the undamaged $K_{n,u}$ and the damaged building $K_{n,d}$,
- determining the degree of damage based on the ratio of the total base shear force at the yield limit of the undamaged building $V_{y,u}$ and the damaged building $V_{y,d}$,
- determining the degree of damage based on the ratio of the total base shear force of the building for the level of hardening/softening of the undamaged $V_{h/s,u}$ and the damaged building $V_{h/s,d}$,
- determining the degree of damage based on the ratio of maximum realized displacement on undamaged $D_{max,u}$ and damaged building $D_{max,d}$,
- determining the degree of damage based on the ratio of the adequate total base shear force of the building for the maximum realized displacement in the undamaged $(V/V_y)_{adeq,u}$ and the damaged building $(V/V_y)_{adeq,d}$,
- determining the degree of damage based on the ratio of maximum realized ductility coefficient in the undamaged $\mu_{max,u}$ and damaged building, $\mu_{max,d}$.

Figure 2 shows the pushover curves and damage coefficients C_d obtained by parametric analysis and based on the pre-defined parameters. The damage coefficient values are in the interval of C_d=[0,100] and they are shown in percentages. If the damage coefficient is C_d=0%, then the building is undamaged; if the damage coefficient is C_d=100%, then the building suffers total damage - it collapses. By increasing the initial coefficient of ductility μ_0, the damage coefficient C_d slightly increases as compared to the

undamaged building model, so that even with μ_0=1, the damage coefficient is C_d=0.6% (figure 2a). However, increasing the initial relative total base shear force of the building to $(V/V_y)_0$=0.6, the damage coefficient increases to C_d=7.5% (figure 2b), so it can be concluded that the sensitivity of the damage coefficient C_d is significantly higher when changing the initial relative total base shear force of the building $(V/V_y)_0$ in comparison with changing initial coefficient of ductility μ_0. By increasing the coefficient of ductility at the yield limit to μ_y=2 (hypothetical) of the damaged building, the damage coefficient increases to C_d=13.2% (figure 2c), while by reducing the relative total base shear force of the building at yield limit to $(V/V_y)_y$=0.4, the damage coefficient increases to C_d=16.1% (figure 2d). High values of coefficient of ductility for the level of hardening/softening $\mu_{h/s}$>6 also lead to higher damage to the building (figure 2e), while with lower $\mu_{h/s}$ values, the damage coefficient C_d is much lower.

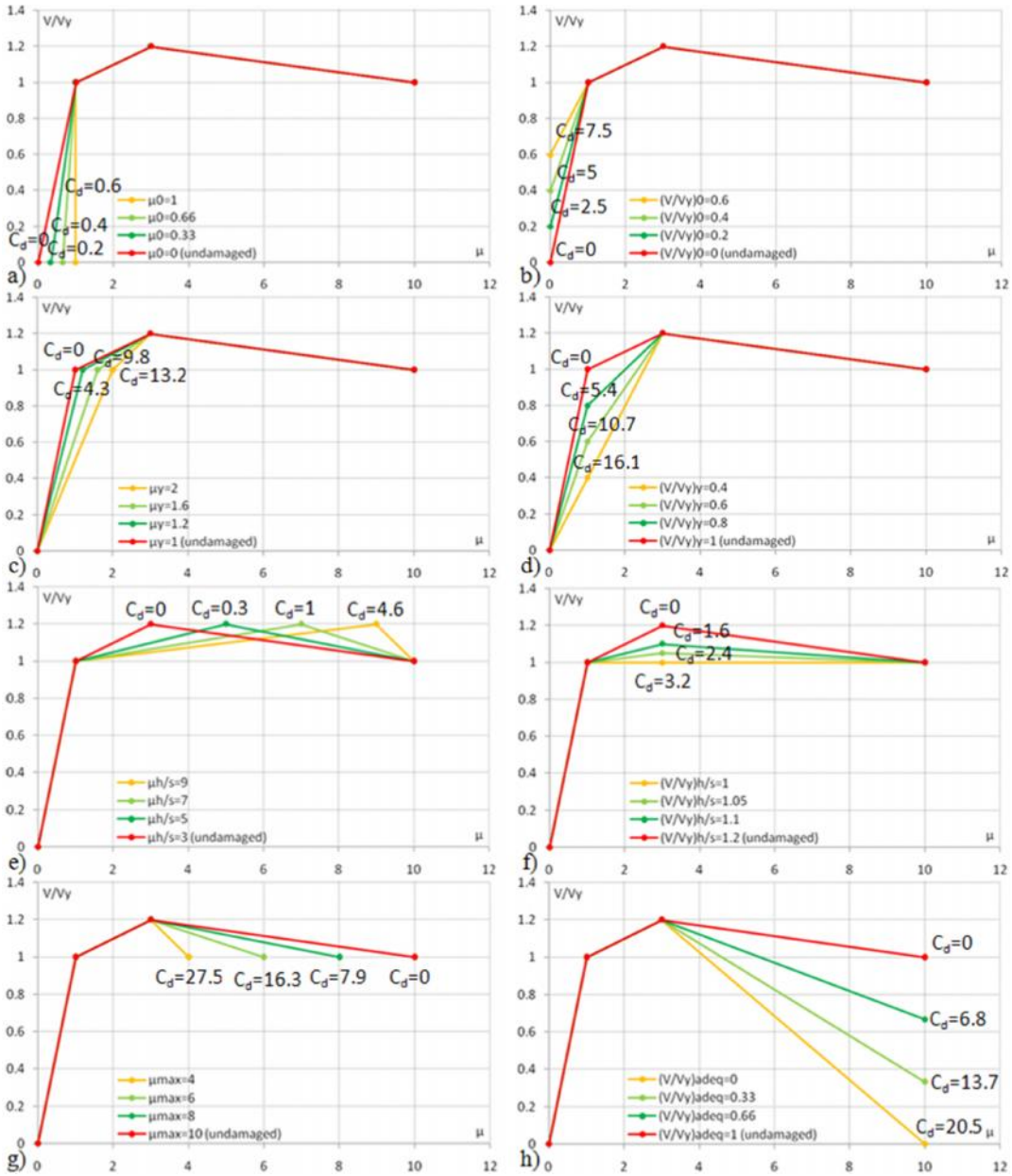

Figure 2. Pushover curves and damage coefficients C_d obtained by parametric analysis: a) initial coefficient of ductility μ_0, b) initial relative total base shear force of the building $(V/V_y)_0$, c) coefficient of ductility at yield limit μ_y, d) relative total base shear force of the building at yield limit $(V/V_y)_y$, e) coefficient of ductility for the level of hardening/softening $\mu_{h/s}$, f) relative total base shear force of the building for the level of hardening/softening $(V/V_y)_{h/s}$, g) coefficient of the maximum realized ductility μ_{max}, h) adequate relative total base shear force of the building $(V/V_y)_{adeq}$ (Ćosić & Folić, 2015)

However, a gradual increase in the relative total base shear force of the building for the level of hardening/softening $(V/V_y)_{h/s}$ also leads to the gradual increase in the damage coefficient C_d, but this increase is not disproportional, as it is the case with $\mu_{h/s}$ (figure 2f). The coefficient of maximum realized ductility μ_{max} and the adequate total relative base shear force of the building $(V/V_y)_{adeq}$ are proven the most sensitive among all analyzed parameters. Figures 2g and 2h show the variation of these parameters and calculated damage coefficients C_d.

PROMETHEE OPTIMIZATION

The PROMETHEE method has been developed for the purpose of multi-criteria decision making in strategic projects, with the best (compromise) solution in multi-criteria terms being determined by (Brans J., Vincke, 1985):

$$\max\left\{g_1(a), g_2(a), \mathrm{K}\ g_j(a), \mathrm{K}\ g_k(a) \middle| a \in A\right\}, \tag{4}$$

where A is the set of permissible alternatives:

$$A = \left\{a_1, a_2, \mathrm{K}\ a_i, \mathrm{K}\ a_n\right\}, \tag{5}$$

G is a set of criteria functions:

$$G = \left\{g_1(\cdot), g_2(\cdot), \mathrm{K}\ g_j(\cdot), \mathrm{K}\ g_k(\cdot)\right\}. \tag{6}$$

The decision maker should identify a single alternative by optimizing each criterion. The basic data on the multi-criteria problem are located in the decision matrix, where each criterion in the decision matrix needs an appropriate weight w_j to be assigned to. The set of assigned criterion weights $\{w_j, j=1, 2,..,k\}$ defines the relative importance of the criterion in the decision-making process. The criterion weight is a positive number which is independent of the unit of measurement of the given criterion. Higher weight values indicate higher importance for the decision-maker. Weights assigned to the criteria should be normalized, i.e. the following equality should hold:

$$\sum_{j=1}^{k} w_j = 1. \tag{7}$$

The PROMETHEE method is based on the comparison of each pair of alternatives across each of the selected criteria, based on which the decision maker has the ability to assign a preference to one of the alternatives, where preferences can take a value in the range between 0 and 1. Higher values in the given interval indicate higher preferences, meaning that the decision maker considers a particular preference function for each criterion. This study uses the criteria of linear preferences with the principle of indifference:

$$P(d) = \begin{cases} 0 & d \le m \\ \dfrac{d-m}{n-m} & m < d < n \\ 1 & d > n \end{cases}, \tag{8}$$

where m is the indifference threshold, n is the strict preference threshold. The preference index for the considered pair of actions (a_i, a_s) is determined by:

$$IP(a_i, a_s) = \sum_{j=1}^{m} w_j P_j(a_i, a_s), \tag{9}$$

while the inbound and outbound flows of action are determined by:

$$\Phi^-(a) = \frac{1}{n-1}\sum_{a \in A} IP(a_s, a_i), \qquad \Phi^+(a) = \frac{1}{n-1}\sum_{a \in A} IP(a_i, a_s). \tag{10}$$

The final solution is obtained by balancing the inbound and outbound flows of actions:

$$\Phi(a) = \Phi^+(a) - \Phi^-(a). \tag{11}$$

NUMERICAL ANALYSIS AND DISCUSSION

Verification of the developed scenario of related non-linear analyses is performed on the example of a 10 storey buildings with a frame static system. In figure 3 are displayed the 3D model and layout of a 10 storey building. Previously the building was designed in compliance with (EN 1992-1-1:2004, 2004) and (EN 1998-1:2004, 2004) codes, taking into consideration the calculation concept according to the

Capacity Design Method. The floor plan dimensions of the building are 36x24m, while the dimensions of a bay are 6x6m. The total height of the building is 33m, but the height of a one storey is 3.3m. The building is designed for concrete class C25/30. From the ground-floor to the fifth storey, the dimensions of the external columns are 50x60cm, and of the internal ones 60x70cm, while from the fifth storey to the tenth storey, dimensions of the external columns are 40x50cm, and of the interior ones 50x60cm. From the ground-floor to the fifth storey, the dimensions of the beams are 35x60cm, and from the fifth storey to the tenth storey they are 30x60cm. The thickness of slabs of all storeys is 20cm. The building load is calculated as a permanent one (dead weight of the structural building elements and the additional permanent load g=3kN/m²), useful (live load p=3kN/m²) and seismic load. The building was designed for the return period of reference seismic action of T=475g, design ground acceleration a_g=0.25g, ground type C, ductility class DCH and behaviour factor q=5.85. Since structural system of the building is formed by columns and beams as linear elements, and slabs as surface elements, such buildings belong to the group of non-stiff and deformable systems. For these systems, it is very important to limit the relative inter-storey drift according to $d_r v \leq 0.01h$, where h is the height of the storey, v is reduction factor which takes into consideration the lower return period of the seismic event and refers to the limit state of serviceability, d_r design inter-storey relative horizontal drift, calculated as the difference between mean horizontal drifts d_s at the top and the bottom of the observed storey (EN 1998-1:2004, 2004). Maximum values of inter-storey drifts are lower than the limit value of the inter-storey drift IDR_{EC8} for v=0.5.

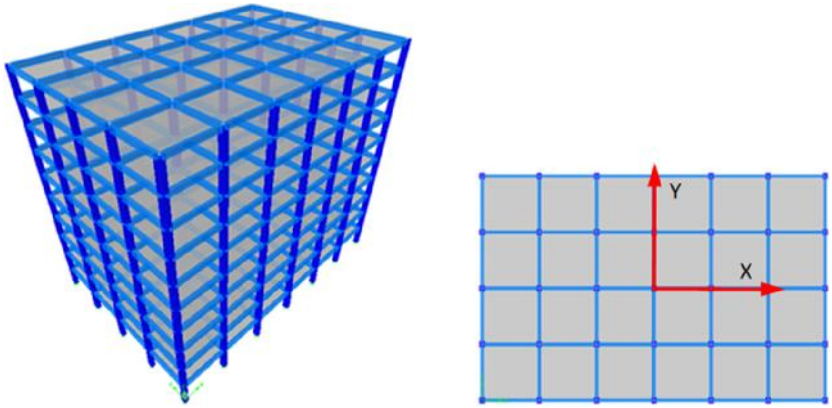

Figure 3. 3D model and layout of the 10-storey building

The scenario of column collapse was conducted by elimination of individual columns of the ground-floor of a 10-storey building. In figure 4 are presented nine scenarios of collapse states of ground-floor columns (or sudden removal corner, edge and internal columns), with the following possible options:

- the scenarios displaying collapse states of outer columns only correspond to the possible damage of these columns due to the terrorist action comprising detonation of explosive in a vehicle parked in the immediate vicinity of the building,
- the scenarios displaying collapse states of inner columns only correspond to the potential damage of these columns due to the terrorist action comprising detonation of explosive planted inside the building,
- the scenarios displaying collapse states of both interior and exterior columns corresponds to the possible damage o these columns due to intensive and simultaneous detonation of explosives planted inside the building.

Material non-linearity is developed through plastic hinges, wherein beams are allowed to plastify under the impact of bending moments, while columns are allowed to plastify under the interaction of the bending moment and normal force. The non-linear behaviour of the buildings for the X direction was considered separately from that considered for the Y direction. In case of the X direction, the displacement of the highest node of the building in the centre of mass for the degree of freedom (DOF) in the X direction was monitored, while in case of the Y direction the displacement of the highest node of the building in the centre of mass for the degree of freedom in the Y direction was monitored. In the

course of performing the NSPA analyses, bidirectional pushover load was assumed for each direction.

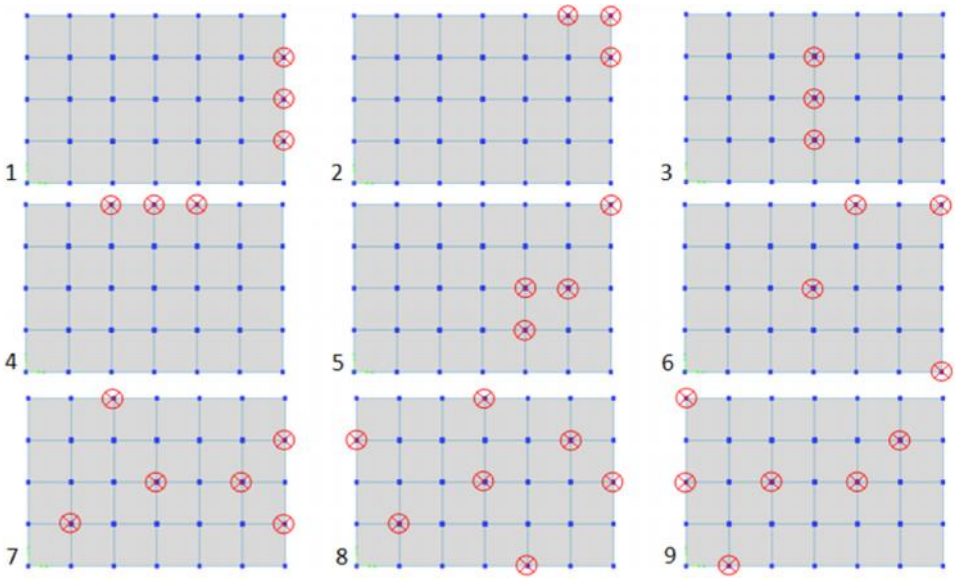

Figure 4. Scenarios of building damage (collapse of ground level columns)

Figure 5 shows NSPA pushover curves for the pre-defined scenarios and undamaged building. By considering the bearing capacity in the non-linear domain, for all NSPA pushover curves, it can be concluded that it is the highest for the undamaged building, which was to be expected. However, from the aspect of realized non-linear displacements, maximum displacements were obtained in the case of the first scenario for the X direction and the fourth scenario for the Y direction. The results obtained in this way describe the vulnerability level of the building in case when only outer columns are damaged. Considering initiation of stiffness in the linear domain, it can be stated that not all the NSPA pushover curves start from the zero. This is the result of application of related non-linear analysis, which assumes that firstly there were collapse states in the columns and then the NSPA analysis was conducted. For such scenarios, the level of initial drift is most frequently shifted towards the positive value. In certain cases, the levels of maximum realized drifts are lower than the maximum realized drifts, which were obtained for undamaged buildings. In such situations, the collapse of the buildings sets in sooner, so the lower the level of maximum realized drift, the sooner the collapse state of the building sets in.

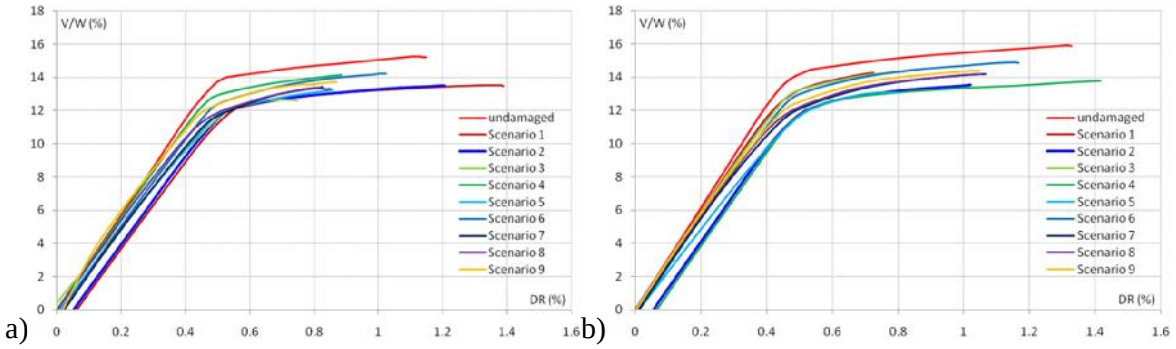

Figure 5. NSPA pushover curves for the pre-defined scenarios: a) monitoring of displacement for the degree of freedom in the X direction, b) monitoring of displacement for the degree of freedom in the Y direction

In the second part are considered global *DR* and inter-storey drifts *IDR* for the maximum realized level of displacement (collapse state). In table 1 are presented the calculated parameters of the maximum realized displacement for the undamaged building and possible scenarios, separately for the X direction and separately for the Y direction. These parameters were conducted according to the CSM (*Capacity*

Spectrum Method) from the (ATC 40, 1996) codes. Apart from the parameters such as: maximum realized displacement D_{max}, total base shear force for the maximum realized displacement V, effective period of vibrations for the maximum realized displacement $T_{eff,max}$ and coefficient of effective damping for the maximum realized displacement $\xi_{eff,max}$, also presented are departures in percents per scenario, in comparison with the model of the undamaged building. The percentages of deviations of $T_{eff,max}$ and $\xi_{eff,max}$ are not uniform (unequivocal), but are both positive and negative since the maximum displacements are reached in the scenarios, which are both higher and lower than the maximum displacements of the undamaged building. The total base shear force for the maximum realized displacement V is lower in all the scenarios in comparison to the V of the undamaged building. The situation is similar for the maximum realized level of displacement D_{max}, except for the first and second scenario of the X directions and fourth scenario of the Y direction.

Table 1. Calculated parameters for the maximum realized displacement (collapse state)

monitoring X DOF								
scenario	D_{max} (cm)		V (kN)		$T_{eff,max}$ (s)		$\zeta_{eff,max}$ (%)	
undamaged	37.9		14970.3		3.29		21.6	
S1	45.9	+21.1%	13275.6	-11.3%	3.67	+11.6%	25.4	+3.3%
S2	39.2	+3.4%	13928.3	-6.9%	3.02	-8.2%	22.4	-8.9%
S3	24.7	-34.8%	12417.1	-17.1%	2.84	-13.7%	19.2	-21.9%
S4	29.9	-21.1%	13273.8	-11.3%	3.48	−5.8%	24.6	0%
S5	28.3	-25.3%	13011.5	-13.1%	3.05	-7.3%	20.6	-16.3%
S6	33.8	-10.8%	13990.0	-6.5%	3.20	-2.7%	23.6	-4.1%
S7	27.2	-28.2%	13206.4	-11.8%	2.95	-10.3%	21.1	-14.2%
S8	28.1	-25.9%	13122.8	-12.3%	3.06	-7.0%	22.3	-9.3%
S9	28.7	-24.3%	13491.5	-9.9%	3.07	-6.7%	22.9	-6.9%
monitoring Y DOF								
scenario	D_{max} (cm)		V (kN)		$T_{eff,max}$ (s)		$\zeta_{eff,max}$ (%)	
undamaged	43.8		15634.8		3.41		24.9	
S1	23.9	-45.4%	14040.0	-10.2%	2.71	-20.5%	18.3	-26.5%
S2	33.7	-23.1%	13303.7	-14.9%	3.14	-7.9%	22.9	-8.0%
S3	27.0	-38.3%	14115.8	-9.7%	2.89	-15.2%	20.7	-16.9%
S4	46.7	+6.6%	13564.0	-13.2%	3.61	−5.9%	25.1	+0.8%
S5	26.1	-40.4%	12875.6	-17.6%	2.88	-15.5%	18.5	-25.7%
S6	38.5	-12.1%	14631.9	-6.4%	3.33	-2.4%	24.5	-1.6%
S7	35.2	-19.6%	13976.1	-10.6%	3.29	-3.5%	23.9	-4.0%
S8	34.7	-20.8%	13949.0	-10.8%	3.28	-3.8%	23.8	-4.4%
S9	34.6	-21.0%	14164.9	-9.4%	3.22	-5.6%	23.7	-4.8%

Global drifts *DR* for maximum realized displacements (collapse state) are determined by:

$$DR_{max,i} = \frac{\left|D_{max,i,j,k,max}\right|}{H_i}, \tag{12}$$

where $DR_{max,i}$ is the global drift for the maximum realized level of displacement of the *i*-th storey, $D_{max,i,j,k,max}$ is maximum displacement of the *j*-th node for maximum realized level of displacement of the *i*-th storey of the *k*-th degree of freedom, H_i is the height of the *i*-th storey from the basement. Inter-storey drifts *IDR* for maximum realized displacement (collapse state) are determined by:

$$IDR_i = \frac{\left|D_{max,i+1,j,k,max}\right| - \left|D_{max,i,j,k,max}\right|}{H_{i+1} - H_i}, \tag{13}$$

where IDR_i is inter-storey drift for maximum realized level of displacement of the *i*-th storey. Figure 6 shows global drifts *DR* for X and Y directions at maximum displacement realized for 3D frame building model. When considering global drifts *DR*, it can be concluded that they are higher in cases of the first and second scenarios in the X direction and the fourth scenario in the Y direction, compared to the global drifts of undamaged building. All other global drifts are smaller. This clearly indicates that collapse states develop much earlier than in undamaged building, except in cases of the first and second scenario in the X direction and the fourth scenario in the Y direction, where the value of ductility is increased, but the bearing capacity of the entire building in the non-linear domain significantly reduced. Figure 7 shows the inter-storey drifts *IDR* in X and Y directions for the maximum realized displacements for the 3D frame

building model. Inter-storey drifts *IDR* also indicate higher values between the ground and the sixth storey in the first and second scenario in the X direction and the fourth scenario in the Y direction. However, all inter-storey drifts above the sixth storey are almost bigger than those in the undamaged building. This clearly points to the fact that in all collapse-state scenarios, higher inter-storey drifts occur at higher storeys. Between the ground and the sixth storey, inter-storey drifts are lower in all scenarios, except for the first and second scenario in the X direction and the fourth scenario in the Y direction, although they also decrease at the ground and first storey. Lower values of inter-storey drifts indicate lower levels of vulnerability of the building's infill walls. However, these values of inter-storey drifts should be considered in correlation with the building's realized global drifts. As already noted, all global drifts are lower than those in the undamaged building, except for the first and second scenario in the X direction and the fourth scenario in the Y direction, so that higher values for these inter-storey drifts can't even be realized since the early appearance of collapse state.

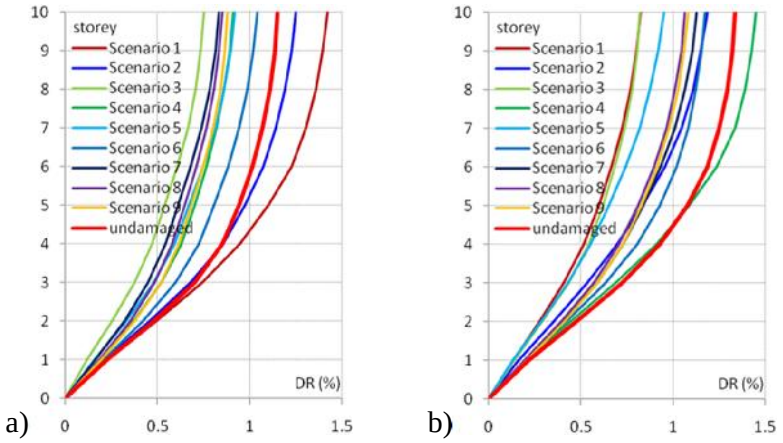

Figure 6. Global drifts *DR* for the maximum realized displacement (collapse state) of the 3D frame building model: a) X direction, b) Y direction

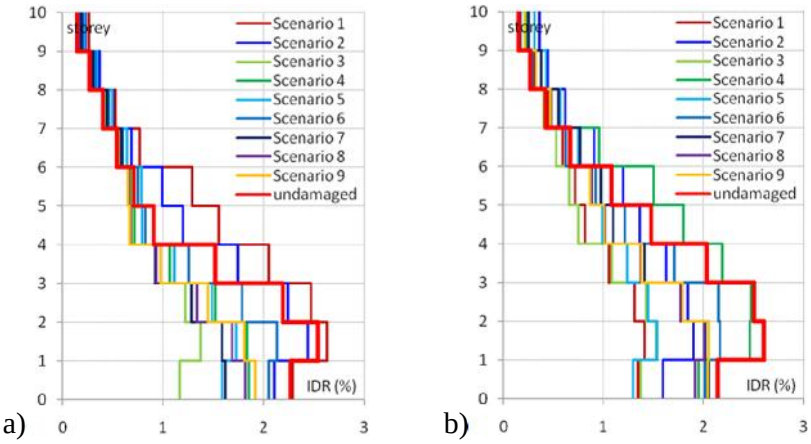

Figure 7. Inter-storey drifts *IDR* for the maximum realized displacements (collapse state) of the 3D frame building model: a) X direction, b) Y direction

In the third part of the research damage coefficients C_d for all pre-defined scenarios were calculated. Figure 8 shows the tri-linear spline interpolated models of the original pushover curves in X direction for the nine pre-defined damage scenarios. Damage coefficients C_d are also presented in percentages. Damage coefficient C_d is the lowest in the case of the first scenario, whereby there is a significant deviation between the damaged and the undamaged building. The value of load bearing capacity in the non-linear domain is reduced and there is an initial displacement due to the collapse of ground-floor columns. However, in this scenario, the value of maximum realized ductility of the damaged building is higher than the value of maximum realized ductility of the undamaged building. This fact indicates that

higher system ductility leads to higher dissipation of hysteresis energy, so that assessed damage to the building is lower. Compared to the first and the second scenario, where higher maximum system ductility values were realized, in other scenarios lower system ductility values were realized. Thus, for example, the highest value of damage coefficient C_d is obtained for the third scenario, given the lowest maximum realized ductility, and the lowest bearing capacity value in the non-linear domain. Figure 9 presents the tri-linear spline interpolated models of original pushover curves in Y direction for nine pre-defined damage scenarios.

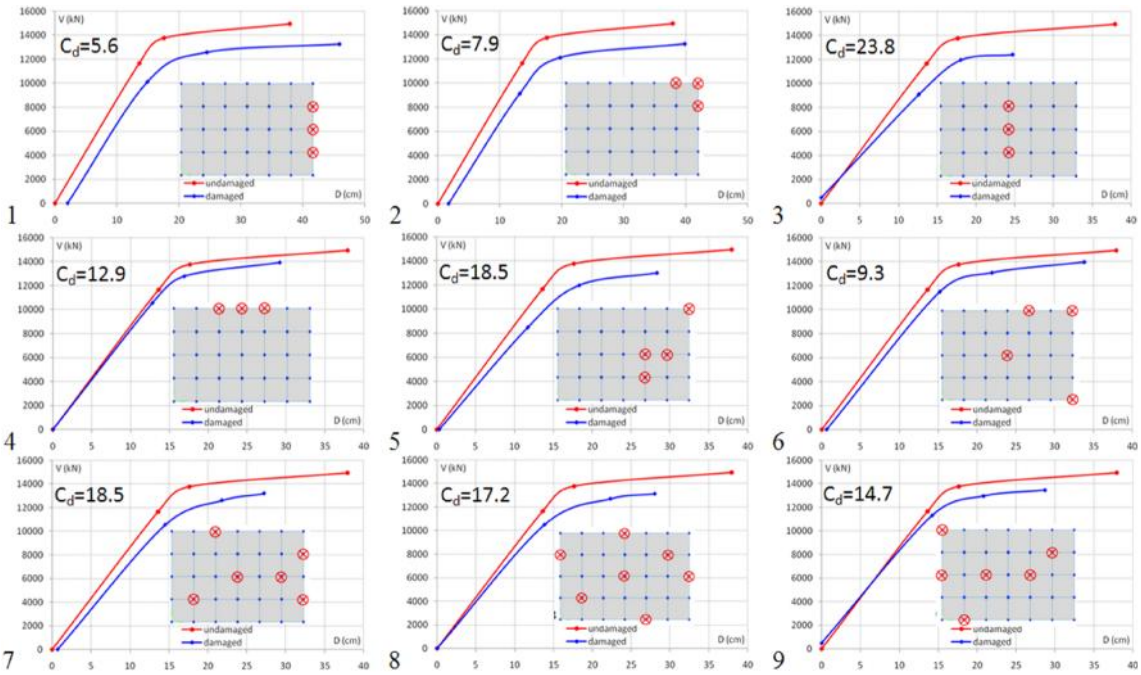

Figure 8. Tri-linear spline interpolated models of original pushover curves in X direction for pre-defined damage scenarios (collapse of the ground-floor columns)

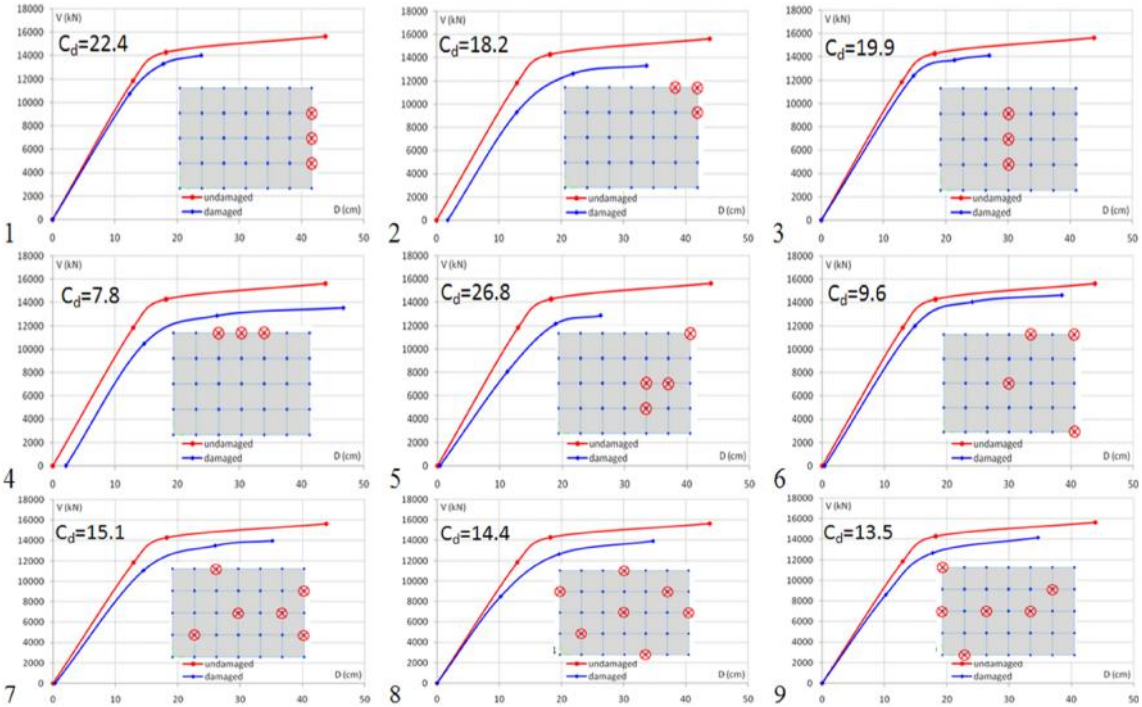

Figure 9. Tri-linear spline interpolated models of original pushover curves in Y direction for pre-defined damage scenarios (collapse of the ground-floor columns)

Damage coefficients C_d are the lowest in the case of the fourth scenario, whereby there is a significant deviation between the damaged and undamaged building. Similar to the case in the first scenario in X direction, the value of the load bearing capacity in the non-linear domain is also reduced and there is also an initial displacement induced by the collapse of ground-floor columns. Compared to the fourth scenario, where higher maximum system ductility values were realized, in other scenarios lower system ductility values were realized. The highest value of damage coefficient C_d is obtained for the fifth scenario, given the lowest maximum realized ductility value, accompanied by reduced bearing capacity of the system in the non-linear domain.

Optimization using the PROMETHEE method was conducted in order to answer the question regarding the priority damage scenario for repair, so that 9 activities were defined for this purpose that correspond to predefined damage scenarios S1÷S9. The following criteria were taken into consideration: maximum global drift DR_{max}, inter-storey drift *IDR* for the level of maximum global drift DR_{max}, and total shear force at the building base *V* for the level of global drift DR_{max}. Given the fact that the drift in the non-linear system response was considered by floors, the criteria were also defined as a function of global and inter-storey drifts for each floor, so that the total number of criteria is 21 (10 DR_{max} criteria across each floor, 10 *IDR* criteria for DR_{max} across each floor, and 1 criterion *V* for DR_{max}). The criteria of maximum global drift DR_{max} were normalized according to:

$$g_j\left(DR_{max}\right) = C_{d,k}\left|DR_{max,i,k} - DR_{max,i,u}\right|, \tag{14}$$

where $DR_{max,i,k}$ is the maximum global drift of the *i*-th floor and *k*-th damage scenario, $DR_{max,i,u}$ is the maximum global drift of the *i*-th floor of the undamaged building, and $C_{d,k}$ is the damage coefficient of the *k*-th scenario. Criteria of inter-storey drift *IDR* for the maximum level of global drift DR_{max} were normalized according to:

$$g_j\left(IDR\right) = C_{d,k}\left|IDR_{i,k} - IDR_{i,u}\right|, \tag{15}$$

where $IDR_{i,k}$ is the inter-storey drift of the *i*-th floor and *k*-th damage scenario for the level of maximum global drift DR_{max}, $IDR_{i,u}$ is the inter-storey drift of *i*-th floor of the undamaged building for the maximum level of global drift DR_{max}. Criteria of the total shear force in the base of the building *V* for the level of global drift DR_{max} was normalized according to:

$$g_j\left(V\right) = C_{d,k}\left|V_{i,k} - V_{i,u}\right|, \tag{16}$$

where $V_{i,k}$ is the total shear force at the base of the building of the *i*-th floor and *k*-th damage scenario for the level of global drift DR_{max}, $V_{i,u}$ is the total shear force in the base of the undamaged building of the *i*-th floor for the level of global drift DR_{max}.

Figure 10 presents the final solutions obtained by the optimization across the maximum global drift DR_{max} (balancing between inbound and outbound flows of actions Φ) for the predefined damage scenarios in X and Y directions by simultaneous calculation. First the situation was discussed in which all the weights assigned to the criteria were equivalent for all floors. This was followed by assigning maximum weight values successively to each criterion of the maximum normalized global drift $g_j(DR_{max})$. Solutions were ranked from the maximum towards the minimum values of the Φ coefficient, where the maximum value of this coefficient indicates a damage scenario which is a priority for repair/strengthening. By analyzing the obtained Φ coefficient and optimizing across the maximum global drift DR_{max} it can be concluded that scenario S3 has the highest priority for repair, followed by scenarios S5 and S7. The maximum value of damage coefficient in X direction is C_d=23.8 (scenario S3), in Y direction C_d=26.8 (scenario S5). Thus, considering the scenario with the highest priority for repair, different solutions are obtained along the X and Y directions, while the applied optimization relates to the consideration of the whole system. The lowest priority for repair is that of solutions S2 and S6.

Figure 11 shows the final solutions obtained by optimizing across the inter-storey drift *IDR* for the maximum level of global drift DR_{max} (balancing the inbound and outbound action Φ) for predefined scenarios for directions X and Y with simultaneous calculation. Similarly to the previous consideration, maximum weight values were successively assigned to each criterion of normalized inter-storey drift $g_j(IDR)$. By analyzing the obtained Φ coefficient and optimizing across the inter-storey drift *IDR*, it can

be concluded that scenario S3 has the highest priority of repair, with scenario S5 having the highest priority in the upper floors. This fact indicates that if determining the inter-storey drift *IDR* is more important than determining the maximum global drift DR_{max}, then the order of priority of scenarios changes. Considering the response and damage to the system through inter-storey drifts is very important from the aspect of vulnerability analysis of the filling or façade cladding, which can be very brittle. Scenarios with the lowest level of priority are S6 and S9. Interestingly, scenario S6 in both calculation situations has the lowest coefficient Φ, even though its damage coefficient values C_d are not the lowest neither in the X nor the Y direction.

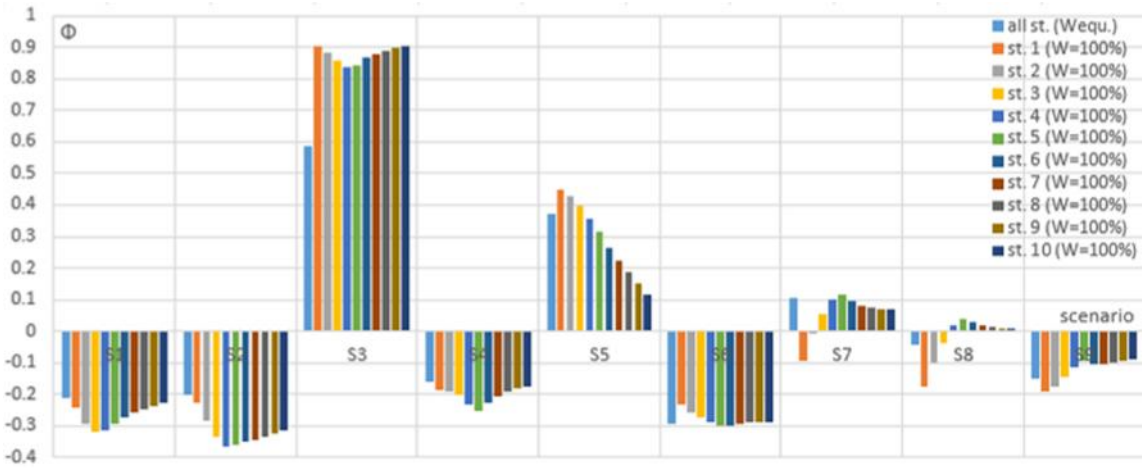

Figure 10. Final solutions obtained by optimizing across the maximum global drift DR_{max} (balancing the inbound and outbound flow of actions Φ) for the predefined scenarios for X and Y directions calculated simultaneously

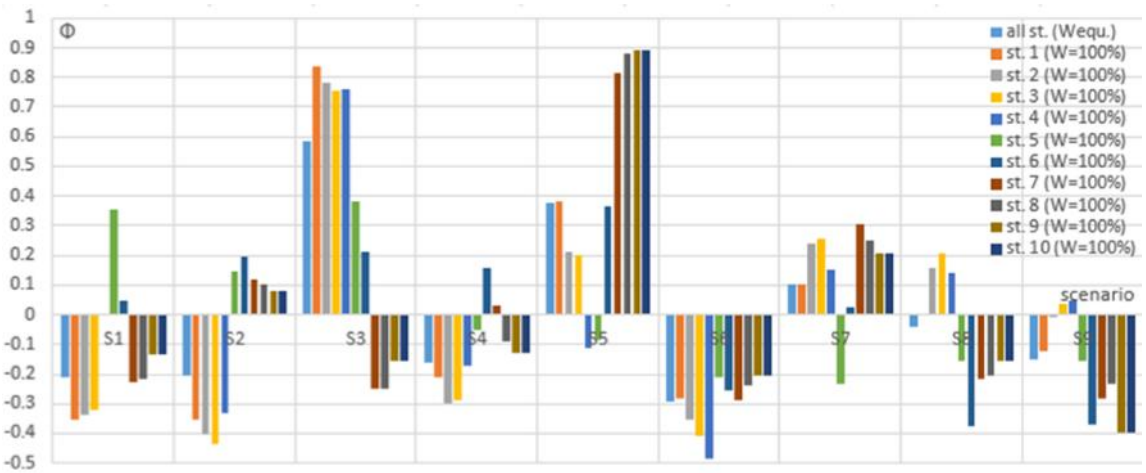

Figure 11. Final solutions obtained by optimizing across the inter-storey drift *IDR* (balancing the inbound and outbound flow of actions Φ) for the predefined scenarios for X and Y directions calculated simultaneously

Figure 12 shows the final solutions obtained by optimizing: only across all maximum global drifts DR_{max} (weight assigned to the criteria are equivalent for all floors), only across all inter-storey drifts *IDR* for the level of maximum global drift DR_{max} (weights assigned to the criteria are equivalent for all floors), and only across the total shear force in the base of the building *V* for the level of global drift DR_{max} (weights assigned to the criteria are equivalent for all floors). Calculations are shown through balancing the inbound and outbound flows of action Φ for the predefined scenarios for both direction X and Y calculated simultaneously. By analyzing the obtained coefficient Φ and optimizing only across all maximum global drifts DR_{max} and across the total shear force in the base of the building *V* for the level of

global drift DR_{max} it can be concluded that scenario S3 has the highest priority of repair, followed by scenarios S5 and S7. In case of analyzing the result obtained by optimizing only across all inter-storey drifts *IDR* for the level of maximum global drift DR_{max}, the highest priority for repair is that of scenario S5, with scenario S6 having the lowest priority.

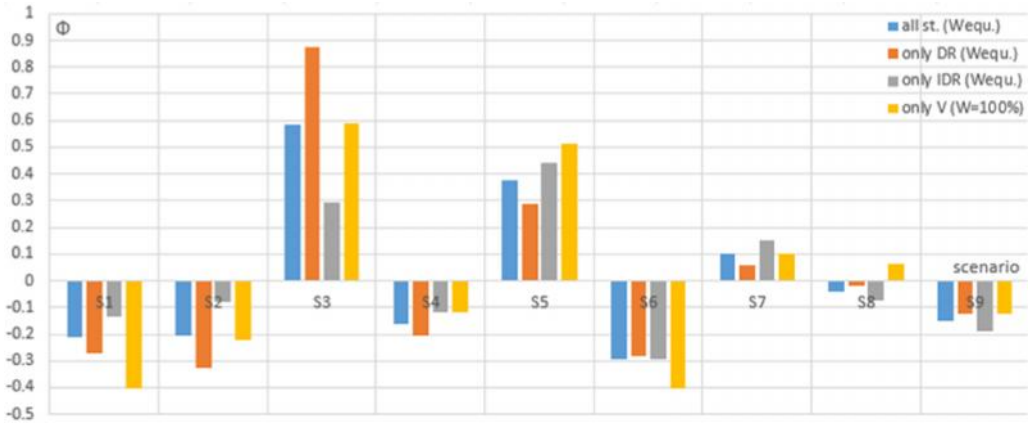

Figure 12: Final solutions obtained by optimization only across all maximum global drifts DR_{max} (weight assigned to the criteria are equivalent for all floors), only across all inter-storey drifts *IDR* for the level of maximum global drift DR_{max} (weights assigned to the criteria are equivalent for all floors), and only across the total shear force in the base of the object *V* for the level of global drift DR_{max} (weights assigned to the criteria are equivalent for all floors)

CONCLUSION

Based on the developed methodology and the non-linear numerical analysis of the 3D building model conducted, it has been concluded that global drifts for the maximum realized displacement (collapse state) may be higher in the undamaged building than global drifts in the damaged-building scenarios. This is due to the fact that in certain damaged-building scenarios the collapse appears much earlier than it is the case with the undamaged building, so higher levels of displacement cannot be realized. Therefore, it is necessary to identify the maximum realized displacement and the building's collapse initiation level. Inter-storey drifts for the maximum realized displacement (collapse state) of the undamaged building can be higher than those of the damaged building, but they should be considered in context with global drifts. In this case, inter-storey drifts were determined for various global drift values, as in almost all damage scenarios significantly lower global drift values were realized, which could have been expected provided that their corresponding inter-storey drifts were lower. However, at higher storeys they were higher for even much lower global drift values than in the undamaged building.

Based on the defined and analyzed damage coefficient, the degree of damage to the system in the capacitive domain can be reliably and quickly identified. It requires only four parameters (the initial state, the yielding state, the level of hardening/softening and the level of maximum displacement) in order to approximate the models of original pushover curves very efficiently and accurately using tri-linear spline interpolation. Generally, it can be concluded that with the collapse of adjacent ground-floor columns, a significant degree of damage to the building can be expected. Thus, the collapse of few columns can lead to critical situation, as compared to some other arrangement with larger number of columns. With the collapse of columns that are not in the near distance, the degree of damage is also lower than in the above case.

Based on the PROMETHEE optimization of the specific model of the building it was determined that emergency repair is required by scenario S3 when the consideration is carried out based on maximum global drifts DR_{max}. When the damage is considered based on the inter-storey drift *IDR* for the level of maximum global drift DR_{max}, then the urgency increases for scenario S5, considering the damage to filling in the upper floors of the building. However, each building model makes an individual problem,

which disables further generalization since solving such a complex problem requires the multi-parameter approach and optimization, as shown by the methodology developed in this research.

ACKNOWLEDGEMENTS

The work reported in this paper is a part of the investigation within the research project TR 36043 supported by the Ministry for Education and Science Republic of Serbia. This support is gratefully acknowledged (Prof. Dr Radomir Folić).

REFERENCES

ATC 40, *Seismic Evaluation and Retrofit of Concrete Buildings*, Vol. 1, Applied Technology Council, Redwood City, USA, 1996.

BIPS 05, *Preventing Structures from Collapsing, to Limit Damage to Adjacent Structures and Additional Loss of Life when Explosives Devices Impact Highly Populated Urban Centers*, Homeland Security, 2011.

Brans J., Vincke Ph.: *A Preference Ranking Organisation Method* (*The PROMETHEE Method for Multiple Criteria Decision-Making*), Management Science, Vol. 31, Iss. 6, 1985.

Ćosić M., Folić R.: *Performance Analysis of Damaged Buildings Applying Scenario of Related Non-Linear Analyses and Damage Coefficient*, Building Materials and Structures, Vol. 58, Iss. 3, 2015. pp. 3-27.

Design of Buildings to Resist Progressive Collapse, Unified Facilities Criteria, Department of Defense, USA, 2013.

EN 1992-1-1:2004, *Eurocode 2: Design of Concrete Structures - Part 1-1: General Rules and Rules for Buildings*, European Committee for Standardization, Belgium, 2004.

EN 1998-1:2004, *Eurocode 8: Design of Structures for Earthquake Resistance – Part 1: General Rules, Seismic Actions and Rules for Buildings*, European Committee for Standardization, Belgium, 2004.

EN 1990:2002/A1:2005, *Eurocode - Basis of Structural Design*, European Committee for Standardization, Belgium, 2005.

EN 1991-1-7:2006, *Eurocode 1: Actions on Structures - Part 1-7: General Actions - Accidental Actions*, European Committee for Standardization, Belgium, 2006.

Kabir G., Sadiq R., Tesfamariam S.: *A Review of Multi-Criteria Decision-Making Methods for Infrastructure Management*, Structure and Infrastructure Engineering, Vol. 10, No. 9, 2014, pp. 1176-1210.

Karlos V., Solomos G.: *Calculation of Blast Loads for Application to Structural Components*, Joint Research Centre, Report EUR 26456 EN, 2013.

Makovička D., Makovička D. Jr.: *Blast Resistant Design of Structure to Terrorist Explosion*, Proceedings of the 9th International Conference on Structural Dynamics, EURODYN 2014, Porto, Portugal, 2014, pp. 3519-3524.

Ngo T., Mendis P., Gupta A., Ramsay J.: *Blast Loading and Blast Effects on Structures - An Overview*, Electronic Journal of Structural Engineering, Special Iss. 2007, pp. 76-91.

Silva P., Lu B., Nanni A.: *Prediction of Blast Loads Based on the Expected Damage Level by Using Displacement Based Method*, Safety and Security Engineering, Vol. 82, 2005, pp. 1-11.

Stewart M., Netherton M., Rosowsky D.: *Terrorism Risks and Blast Damage to Built Infrastructure*, Natural Hazards Review, Vol. 7, Iss. 3, 2006, pp. 114-122.

Zolghadr H., Izzuddin B., Nethercot D., Donahue S., Hadjioannou M., Williamson E., Engelhardt M., Stevens D., Marchand K., Waggoner M.: *Robustness Assessment of Building Structures under Explosion*, Buildings, Vol. 2, Iss. 4, 2012, pp. 497-518.